Coordination Environment Prevents Access to Intraligand Charge-Transfer States through Remote Substitution in Rhenium(I) Terpyridinedicarbonyl Complexes

Fernández-Terán, Ricardo J ; Sévery, Laurent

Abstract: Six rhenium(I) 3N-dicarbonyl complexes with 4 -(4-substituted phenyl)terpyridine ligands were evaluated in their ground and excited states. These complexes, bearing substituents of different electron-donating strengths—from CN to NMe2—were studied by a combination of transient IR (TRIR), electrochemistry, and IR spectroelectrochemistry, as well as time-dependent density functional theory (TD-DFT). They exhibit panchromatic absorption and can act as stronger photoreductants than their tricarbonyl counterparts. The ground- and excited-state potentials, absorption maxima, and lifetimes (250–750 ps) of these complexes correlate well with the Hammett p substituent constants, showing the systematic effect of remote substitution in the ligand framework. TRIR spectroscopy allowed us to assign the lowest singlet and triplet excited states to a metal-to-ligand charge-transfer (MLCT) character. This result contrasts our previous report on analogous 2N-tricarbonyl complexes, where remote substitution switched the character from MLCT to intraligand charge transfer. With the help of TD-DFT calculations, we dissect the geometric and electronic effects of coordination of the third pyridine, local symmetries, and increasing conjugation length. These results give valuable insights for the design of complexes with long-lived triplet excited states and enhanced absorption throughout the visible spectrum, while showcasing the boundaries of the excited-state switching strategy via remote substitution.

DOI: https://doi.org/10.1021/acs.inorgchem.0c02914

Coordination Environment Disables Intraligand Charge-Transfer States Accessed Through Remote Substitution in Rhenium(I) Terpyridine Dicarbonyl Complexes

Ricardo J. Fernández-Terán* and Laurent Sévery
Department of Chemistry, University of Zurich. Winterthurerstrasse 190, CH-8057 Zurich, Switzerland

*Corresponding Author: Ricardo.FernandezTeran@gmail.com and Ricardo.Fernandez@chem.uzh.ch
(Dated: November 9, 2020)

Abstract: Six rhenium(I) κ^3N-dicarbonyl complexes with 4'-(4-substituted-phenyl)-terpyridine ligands were evaluated in their ground and excited states. These complexes, bearing substituents of different electron-donating strengths—from CN to NMe_2—were studied by a combination of transient IR, electrochemistry and IR spectroelectrochemistry, as well as time-dependent density functional theory (TD-DFT). They exhibit panchromatic absorption and can act as stronger photoreductants than their tricarbonyl counterparts. The ground- and excited-state potentials, absorption maxima and lifetimes (250–750 ps) of these complexes correlate well with the Hammett σ_p substituent constants, showing the systematic effect of remote substitution in the ligand framework. Transient IR spectroscopy allowed us to assign the lowest singlet and triplet excited states to a metal-to-ligand charge transfer (MLCT) character. This result contrasts our previous report on analogous κ^2N-tricarbonyl complexes, where remote substitution switched the character from MLCT to intraligand charge transfer (ILCT). With the help of TD-DFT calculations, we dissect the geometric and electronic effects of coordination of the third pyridine, local symmetries, and increase in the conjugation length. These results give valuable insights for the design of complexes with long-lived triplet excited states and enhanced absorption throughout the visible spectrum, while showcasing the boundaries of the excited-state switching strategy via remote substitution.

INTRODUCTION

Rhenium(I) carbonyl complexes have found widespread applications in chemistry, ranging from their ubiquitous role as photosensitisers in diverse photocatalytic transformations,[1–12] to their use as CO_2 reduction catalysts.[13–18] Complexes of the type *fac*-$[Re(N\wedge N)(CO)_3L]^+$ (where N∧N is a bidentate diimine ligand) have been studied to a great extent, since the pioneering work by Wrighton and co-workers,[19–21] as well as Lehn and co-workers.[22]

While the photochemical and photophysical properties of *fac*-tricarbonyl Re(I) complexes have been studied extensively,[19,23–31] those of mononuclear *cis*-dicarbonyl Re(I) complexes, in contrast, remain to date relatively unexplored.[32] The groups of Castellano,[33] and Sullivan,[34] have recently reported on substituent effects in Re(I) bis-diimine dicarbonyl complexes with general formula $[Re(N\wedge N)_2(CO)_2]^+$, Figure 1A. In addition, Ishitani and co-workers[35] have reported on supramolecular assemblies of Re(I) dicarbonyl complexes with phosphine ligands. Furthermore, Dempsey and co-workers[36] have reported on a series of Re(I) bipyridine dicarbonyl complexes with axial ligands of different donating strengths (Figure 1B), exhibiting broadband visible absorption and acting as stronger photoreductants than conventional Re(I) tricarbonyl complexes. Hightower and co-workers,[37,38] as well as Richeson and co-workers[39] have shown that *cis*-dicarbonyl Re(I) complexes of nitrogen donor ligands bearing a κ^3N coordination motif exhibit enhanced absorption properties throughout the entire visible spectrum—a common feature of these complexes that makes them attractive candidates for applications in photochemical energy conversion.

We have recently reported on a complementary remote substitution strategy to tune the photophysical and photochemical properties of Re(I) tricarbonyl complexes, using a ligand framework based on bidentate 4'-(4-R^1-phenyl)-2,2':6',2"-terpyridine (terpy) ligands (Figure 1C), decorated with electron-withdrawing and donating substituents (ranging from CN to NMe_2).[40] In the present work, we extend our approach to their Re(I) *cis*-dicarbonyl analogues (Figure 1D).

We report herein the synthesis, spectroscopic, crystallographic and electrochemical characterisation of a series of Re(I) κ^3N-dicarbonyl complexes (**3a-f**, Scheme 1) with substituted terpy ligands ($\mathbf{L_a}$-$\mathbf{L_f}$). The present study brings new insights into the photophysical and photochemical properties of this family of complexes. By combining experimental and computational methods, including UV pump-IR probe, FT-IR spectroelectrochemistry, and time-dependent density functional calculations (TD-DFT), we establish herein the key differences between the photophysics of the κ^2N-tricarbonyl and κ^3N-dicarbonyl terpy frameworks.

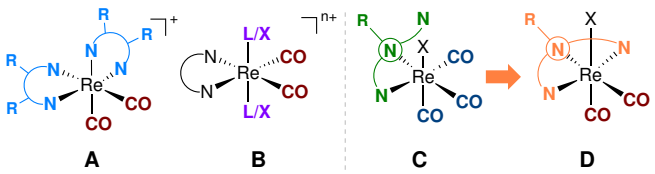

Figure 1. Different strategies for tuning the properties of Re(I) carbonyl complexes: (A) by substitution on the diimine ligands; (B) by tuning the axial ligands; (C) by remote substitution in tricarbonyl complexes and (D) in their dicarbonyl analogues with a terpy framework.

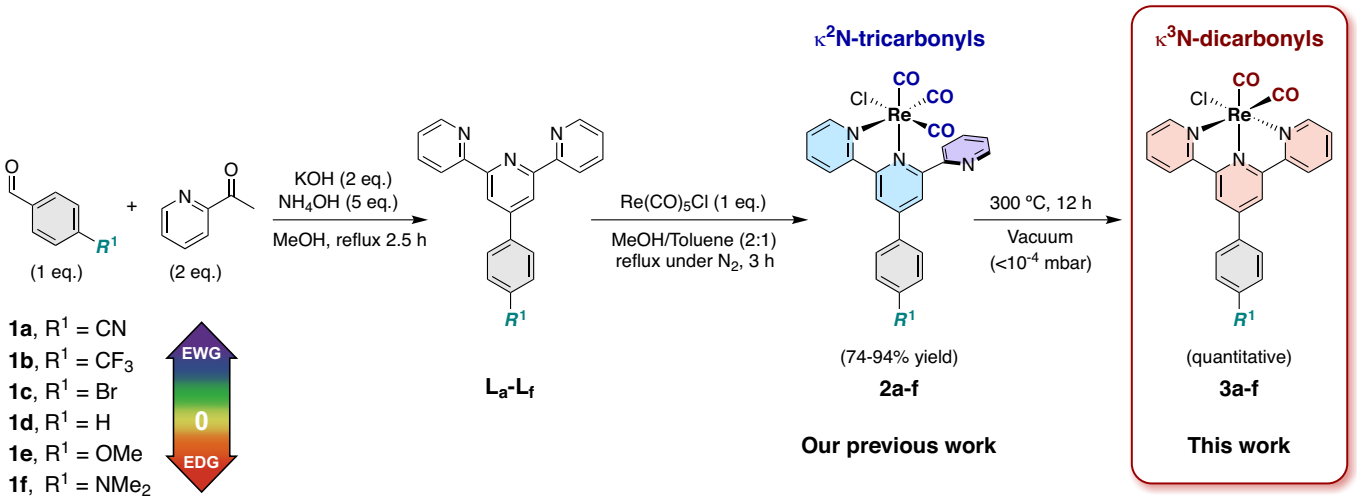

Scheme 1. Synthetic route and structures of the compounds studied in the present work.

We assess the impact of the different coordination geometries and local symmetries around the Re(I) centre, and correlate the observed properties with the electronic density on the terpyridine ligand. These two complementary approaches (i.e. remote substitution and coordination geometry) provide full control over the absorption properties of these complexes, while allowing us to look at their excited-state structure and dynamics.

RESULTS AND DISCUSSION

Synthesis and Characterisation

The synthetic route to the κ^3N-dicarbonyl complexes is shown in Scheme 1. In our previous report,[40] we have described the synthesis of the ligands (**L_a-L_f**, based on a modified Kröhnke strategy with 4-acetylpyridine and a 4-substituted benzaldehyde derivative);[41,42] as well as the synthesis of the κ^2N-tricarbonyl complexes (**2a-f**, obtained from $Re^I(CO)_5Cl$ and the corresponding ligand).

The κ^3N-dicarbonyl complexes studied in this work (**3a-f**) were obtained as air-stable black solids in quantitative yields by thermal decarbonylation of **2a-f** under vacuum (Scheme 1), an improved protocol respect to previous literature reports.[37–39] The key aspect to quantitative conversion is heating the complexes under vacuum (instead of under inert atmosphere), as this is expected to promote CO loss. Complete experimental details are provided in the Supporting Information (SI).

It is worth mentioning that both the κ^2N-tricarbonyl and the κ^3N-dicarbonyl complexes show remarkable photochemical and thermal stability. In comparison, Mn(I) tricarbonyl complexes with terpyridine ligands readily release CO upon photoexcitation, forming the corresponding κ^3N-dicarbonyl complex.[43]

The crystal structures of these complexes (illustrated by that of **3f**, Figure 2) confirm the *mer,cis-* coordination geometry around the Re(I) centre. In the complexes studied in the present work, the plane of $\{Re(CO)_2\}^+$ moiety is almost perpendicular to the plane of the terpyridine ligand, in contrast to other reports of Re(I) dicarbonyl complexes, where the two CO groups are coplanar with the bis-diimine ligand.[36] The N5-Re1-N15 angles close to 150° indicate a slight distortion from ideal octahedral geometry. In general, bond lengths and angles are in line with those of previously reported for similar complexes.[34,44–47] Additional crystallographic details are given in the SI.

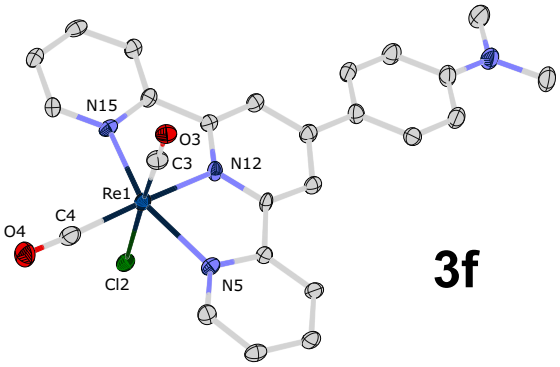

Figure 2. Displacement ellipsoid representation (at the 50% probability level) of the crystal structure of complex **3f**. Hydrogen atoms and disorder omitted for clarity.

The ^{1}H-NMR spectra of all κ^3N complexes (**3a-f**) show a single set of 7 signals for the terpyridine ligand framework, also in agreement with the crystallographically observed *mer,cis-*(κ^3N-terpy) coordination geometry and an apparent C_s symmetry around the Re(I) centre. The chemical shifts of the 3' and 5' protons of the tpy ligand show a linear correlation with the Hammett σ_p substituent constants, suggesting good electronic communication between the ligand subunits. A similar correlation was also observed for the ^{13}C-NMR shifts of the equatorial carbonyl ligands of the κ^3N complexes. The NMR spectra of all complexes are given in the SI.

Steady-State Spectroscopic Properties

Compared to their κ^2N-tricarbonyl counterparts, the κ^3N-dicarbonyl complexes show panchromatic absorption (throughout the entire visible spectrum), manifested in three strong metal-to-ligand charge transfer (MLCT) bands around ca. 720, 480, and 410 nm (denoted herein as ν_1, ν_2, and ν_3, respectively), accompanied by a shoulder around 575 nm (Figure 3A).

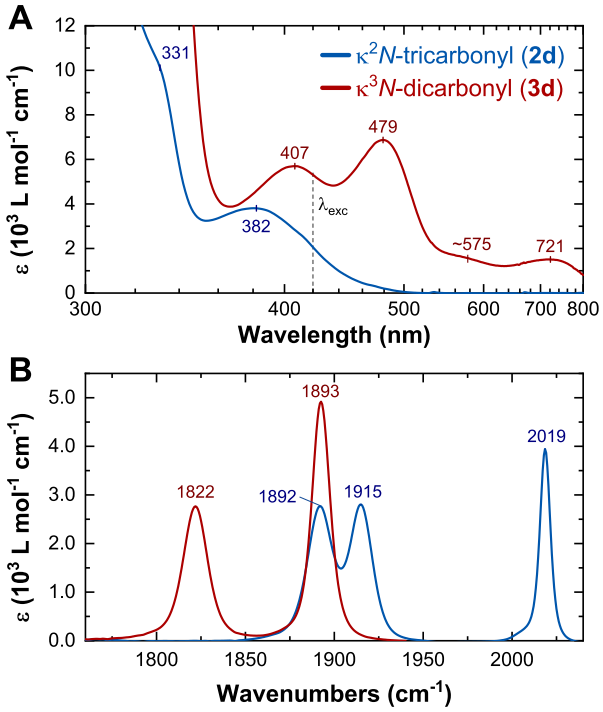

Figure 3. (A) UV-Vis and (B) Fourier-transform infrared (FT-IR) absorption spectra in DMF of the unsubstituted κ^2N-tricarbonyl (**2d**, blue) and κ^3N-dicarbonyl (**3d**, red) complexes.

In the IR, the change from the *fac*-$\{Re(CO)_3\}^+$ to the *cis*-$\{Re(CO)_2\}^+$ moiety leads to an average red shift of ca. 85 cm^{-1} in the CO frequencies (i.e. average of all CO stretching frequencies). The two ν_{CO} absorption bands expected for the *cis*-dicarbonyl complexes are observed around ca. 1820 and 1895 cm^{-1} (Figure 3B).

These two vibrations have, respectively, antisymmetric and symmetric characters (formally both of A' symmetry in the C_s point group)—consisting of out-of-phase and in-phase stretching of the two CO groups, respectively. They preserving the large delocalisation of the C≡O stretching modes observed in their tricarbonyl counterparts.[48] The red shift in the absorption frequencies can be explained by a significant increase in the electron density around the metal centre due to the replacement of an electron-accepting CO group by a donating imine group (from the now meridionally-coordinated terpyridine ligand).

Complexes **3a-e** show consistent hypsochromic (blue) shifts in all UV-Vis absorption maxima as the electron donating character of the substituent is increased—shifting by 614 (ν_1), 390 (ν_2), and 700 cm^{-1} (ν_3), respectively, going from CN to OMe—accompanied by a slight increase in extinction coefficients. These shifts are similar to those observed for **2a-e**. Complete UV-Vis and IR spectra are provided in the SI (Figs. S1-S2).

In contrast to its tricarbonyl counterpart, the NMe_2-substituted complex (**3f**) does not show any significant new bands in its UV-Vis absorption spectrum. The positions (in cm^{-1}) of the the lowest energy band (ν_1) of the UV-Vis spectra show an excellent linear correlation with the Hammett σ_p substituent constants ($R^2 = 0.9983$, Figure S3 in the SI), while those of ν_2 and ν_3 deviate from linearity for the extremely donating or withdrawing substituents.

Complexes **3a-f** are non-emissive—neither at room temperature nor at 77 K, in contrast to their κ^2N-tricarbonyl analogues (**2a-f**). We attribute this to a faster non-radiative deactivation due to the significantly red-shifted absorption (as expected from the energy gap law).

Ground and Excited-State Redox Properties

Electrochemical studies of these complexes were carried out in 0.1 M $[Bu_4N][PF_6]$ in DMF (Figure 4). The κ^3N-dicarbonyl complexes show a one-electron chemically reversible oxidation around ~0 V vs $Fc^{+/0}$, and a stepwise two-electron reduction below –1.5 V vs $Fc^{+/0}$, analogous to that observed in their κ^2N-tricarbonyl analogues.[40] The dicarbonyl complexes show, however, a more evident separation of the two overlapping consecutive reduction waves, especially on the more electron-rich complex **3f**.

The partial irreversibility of the second reduction is attributed to loss of the chloride ligand. This was well reproduced in the DFT calculations, performed in *Gaussian* 16 rev. B.01,[49] and in agreement with previous reports of related complexes.[50–52] The redox potentials of the oxidative and reductive events shift to more negative values with more electron-donating substituents. Peak shifts of –160 and –60 mV were recorded for the reduction and oxidation waves, respectively, between CN and NMe_2 as substituents (Figure S4 in the SI). The ground- and excited-state redox properties of these complexes are summarised in Table I, and discussed below.

Any potential application of these complexes for photoinduced electron transfer reactions requires knowledge of their excited-state redox potentials, which can be estimated by Eqs. 1–2:

$$E^{\circ\prime}_{red}(^3[Re^I]^*) = E^{\circ\prime}_{red} + \Delta G_{ST} \quad (1)$$

$$E^{\circ\prime}_{ox}(^3[Re^I]^*) = E^{\circ\prime}_{ox} - \Delta G_{ST} \quad (2)$$

Since the κ^3N complexes are non-emissive, we estimated the ΔG_{ST} values of these complexes directly from the energy differences between the optimised ground and lowest triplet excited state structures (without further corrections). We base this approach on the excellent

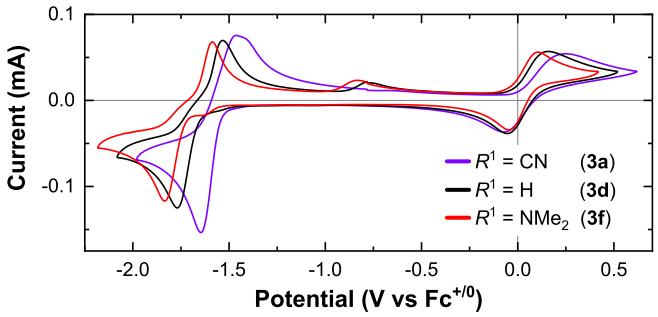

Figure 4. Cyclic voltammograms of selected dicarbonyl complexes in 0.1 M $[Bu_4N][PF_6]$ in DMF. Scan rate: 100 mV s^{-1}.

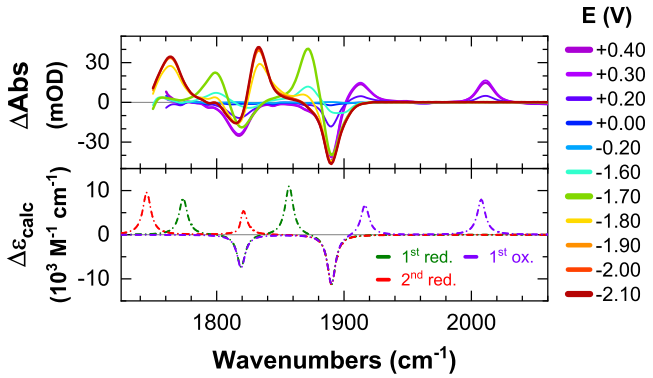

Figure 5. Experimental (*solid lines*) and calculated (*dashed lines*) difference IR spectra of the redox states of **3d**. Experimental spectra measured in 0.1 M $[Bu_4N][PF_6]$ in DMF. Potentials vs $Fc^{+/0}$. Theoretical frequencies were scaled by 0.969 to better match the experimentally obtained values.

agreement between experimental and calculated obtained in our previous report for the $\kappa^2 N$ complexes (with a mean deviation of ±0.02 eV for complexes **2a-e**, operating from a lowest ^{3}MLCT state).[40] Considering the reported $(E^{\circ\prime}_{ox})^*$ values for Re(I) tricarbonyl complexes (≈ 1 V vs Fc^+/Fc in MeCN),[36] we conclude that the $\kappa^3 N$ complexes are stronger photo-reductants but weaker photo-oxidants than their $\kappa^2 N$ analogues.

TABLE I. Ground- and excited-state redox properties of the studied complexes in DMF

	R^1	$E^{\circ\prime}_{red}$ (V)[a]	$E^{\circ\prime}_{ox}$ (V)[a]	$\Delta G^{(theo)}_{ST}$ (eV)[b]	$(E^{\circ\prime}_{red})^*$ (V)[c]	$(E^{\circ\prime}_{ox})^*$ (V)[c]
3a)	CN	–1.58	0.09	1.35	–0.19	–1.26
3b)	CF_3	–1.60	0.07	1.39	–0.20	–1.32
3c)	Br	–1.62	0.06	1.42	–0.20	–1.36
3d)	H	–1.65	0.05	1.44	–0.21	–1.39
3e)	OMe	–1.67	0.05	1.47	–0.19	–1.42
3f)	NMe_2	–1.71	0.03	1.51	–0.20	–1.48

[a] Electrochemical potential in V vs $Fc^{+/0}$ in DMF.
[b] Energy difference between the optimised S_0 and T_1 structures.
[c] Excited-state potentials estimated from Eqs. 1–2.

Spectroelectrochemical studies in the IR (IR-SEC) revealed the absorption features of the singly oxidised, as well as the singly and doubly reduced species. The experimental and calculated IR-SEC difference spectra of **3d** (as a representative example) are shown in Figure 5.

Upon oxidation, the antisymmetric and symmetric CO stretches blue shift by ca. 95 and 120 cm^{-1}, respectively. Similarly, upon reduction both carbonyl stretching bands exhibit red shifts of ∼18 cm^{-1} (first reduction) and ∼55 cm^{-1} (second reduction). Ishitani, Turner and co-workers reported red shifts of 27 and 33 cm^{-1} for the first reduction, and red shifts of 55 and 66 cm^{-1} for the second (irreversible) reduction of *cis,trans*-$[Re(CO)_2(bpy)\{P(OEt)_3\}_2]^+$.[51] In a similar fashion, Hartl and Vlček observed blue shifts of 78 and 92 cm^{-1} (for the first oxidation), and red shifts of 42 and 53 cm^{-1} (for the first reduction) for a Re(I) dicarbonyl diphosphine complex with a quinone ligand.[50]

We tentatively conclude that complexes **3a-f** undergo similar structural changes upon reduction as their tricarbonyl counterparts (**2a-f**),[40,53] leading to Cl^- dissociation after the second reduction. DFT optimisation of the structure of the doubly reduced species also led to dissociation of the Cl ligand. In this case, the doubly reduced complexes were re-optimised by manually removing the Cl ligand.

Overall speaking, the shifts observed upon electrochemical oxidation and reduction of **3a-f** correlate well with those of similar complexes, being significantly higher for the one-electron oxidation. These shifts were almost quantitatively reproduced in DFT calculations of the different redox states, allowing us to safely assign them as described above.

Excited-State Dynamics

We now turn to the excited-state dynamics of complexes **3a-f**. Transient absorption experiments were performed with UV pump and ultrashort broadband mid-IR pulses derived from a home-built OPA as the probe (Complete experimental details are given in Section 1.3 of the SI).[54–56] Transient IR (TRIR) spectra of the complexes **3a-f** in air-saturated DMF were recorded upon excitation with 420 nm ultrashort pulses, and are illustrated in Figure 6 by those of **3d** as a representative example. Overall, the TRIR spectra of all complexes show two excited-state absorption (ESA) bands, centred around 1871 and 1970 cm^{-1}, and the corresponding ground-state bleach signatures at 1820 and 1890 cm^{-1}.

(TD-)DFT calculations of the TRIR spectroscopic signatures for these complexes almost quantitatively matched the experimental TRIR spectra (Figure 7). Based on this, we assigned the observed spectroscopic signatures to population of the lowest ^{3}MLCT state of the $\kappa^3 N$-dicarbonyl complexes after ultrafast intersystem crossing (ISC) and/or internal conversion from an initially populated higher singlet excited state. Evidence for this assignment comes from the pronounced time-

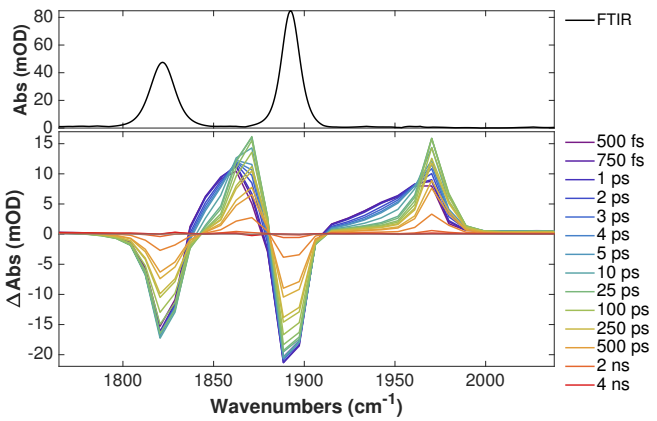

Figure 6. FT-IR spectrum (*top*) and magic-angle TRIR spectra (*bottom*) of **3d** (5 mM in DMF) at different pump-probe delays.

dependent blue shift of the two excited-state absorption bands (also reproduced in the DFT calculations, Figure 7A-B). This process, taking place on a timescale of ca. 10 ps, is attributed to a convolution of relaxation on the excited state(s) (internal conversion) and ISC, analogous to that observed for Re(I) tricarbonyl complexes.[28,57,58]

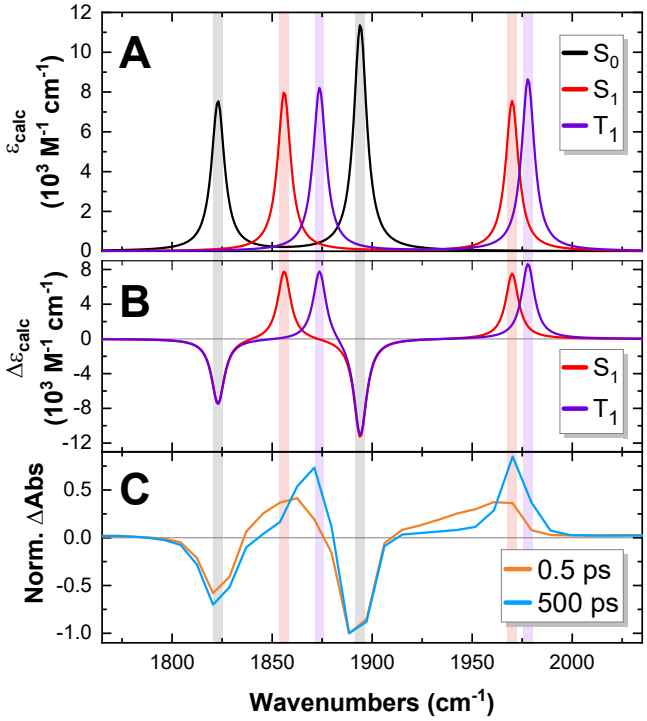

Figure 7. Calculated (A) absolute and (B) difference spectra of the ground and lowest singlet and triplet excited states; (C) Experimental TRIR spectra at early and late population delays. All spectra correspond to **3d** in DMF. Calculated frequencies were scaled by 0.971 to better match the experiment. Vertical coloured bars indicate the positions of the calculated (scaled) frequencies for each state.

It is important here to emphasise that excitation with 420 nm initially populates higher singlet excited states in the $\kappa^3 N$-dicarbonyl complexes. According to TD-DFT calculations, all of these excited states (up to at least S_5) have an MLCT character, irrespective of the substituent on the ligand scaffold. This sharply contrasts the excited-state character switching observed with the NMe_2 substituent in the $\kappa^2 N$-tricarbonyl complexes from our previous report.[40]

The excellent agreement between the experimental and calculated UV-Vis absorption spectra (Figure S5 in the SI) shows that our computational approach accurately reproduces the ground- and excited-state properties.

Considering current and previous observations on Re(I) $\kappa^2 N$-tricarbonyl complexes, we conclude that the photophysics of $\kappa^3 N$-dicarbonyl complexes follow a very similar pathway: excitation to one of the ^{1}MLCT states leads to ultrafast internal conversion and ISC to the lowest-lying ^{3}MLCT state, independent of the substituent on the terpy ligand framework.

Time-resolved investigations of mononuclear Re(I) dicarbonyl complexes are relatively scarce in literature. Ishitani, Turner and co-workers have reported on the photophysical and photochemical properties of *cis,trans*-$[Re(CO)_2(bpy)\{P(OEt)_3\}_2]^+$.[51] In their work, they showed that upon photoexcitation, the ν_{CO} antisymmetric (lower energy) and symmetric (higher energy) bands of this complex blue shift by ca. 45 and 56 cm^{-1}. Similarly, Castellano and co-workers observed blue shifts of ca. 40 and 75 cm^{-1} upon photoexcitation of dicarbonyl Re(I) complexes with substituted bis(diimine) ligands.[33] In the excited ^{3}MLCT state, complexes **3a-f** display a blue shift of the CO stretching bands of ca. 49 and 77 cm^{-1}, in line with previous reports for similar complexes.

We observe, across the series of complexes **3a-f**, a systematic modification of the lifetimes of the lowest triplet excited state (Figure 8), analogous to that observed for **2a-e**. The lifetimes increase from 251 to 762 ps between the CN- and OMe-substituted complexes, up to a maximum of 947 ps for the NMe_2-substituted complex (**3f**) The fitted lifetimes of all complexes can be found on Table S2, and the corresponding TRIR kinetic traces in Figure S6 of the SI.

When comparing the slopes of the lifetimes vs Hammett σ_p substituent constants, we observe that the change for $\kappa^2 N$-tricarbonyl complexes (**2a-e**) is more prominent than that of the $\kappa^3 N$-dicarbonyl complexes (**3a-f**). This results intriguing, considering that both series evidence similar spectral shifts upon substitution (717 and 614 cm^{-1}, respectively, when going from CN to OMe), excluding the NMe_2 complexes.

Computational Aspects

We now turn to TD-DFT calculations to rationalise the observed properties and the differences between the $\kappa^2 N$-tricarbonyl complexes and their $\kappa^3 N$-dicarbonyl counter-

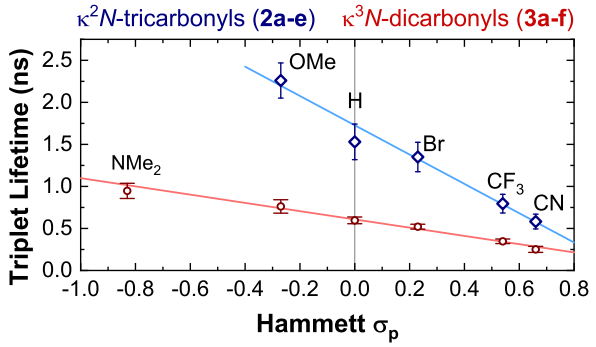

Figure 8. Linear correlations between the ^{3}MLCT lifetimes (from TRIR) and the Hammett σ_p substituent constants for the κ^2N-tricarbonyl complexes (**2a-e**, in blue; **2f** excluded for clarity), and κ^3N-dicarbonyl complexes (**3a-f**, in red).

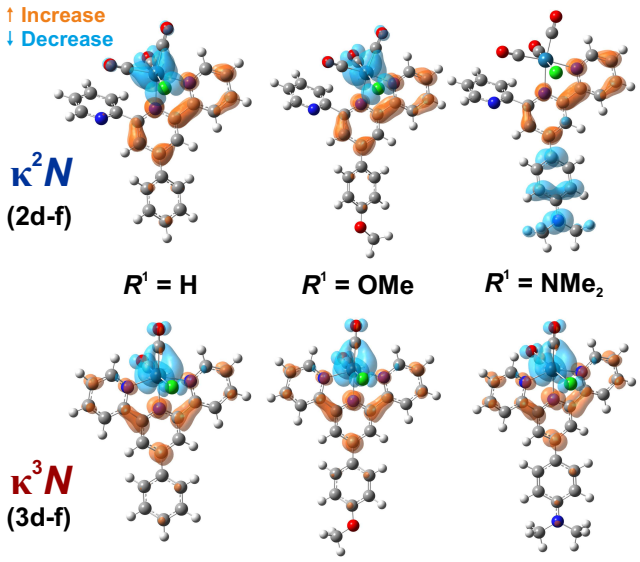

Figure 9. Charge density difference (CDD) isosurfaces of the $S_1 \leftarrow S_0$ transition of complexes **2d-f** (top row) and **3d-f** (bottom row), shown at $|\Delta\rho| = 0.002$ a.u.

parts.

Neither the energy levels of the lowest unoccupied molecular orbital (LUMO), nor those of the highest occupied molecular orbital (HOMO) of complexes **3a-f** correlate with the electron donating/withdrawing properties of the substituents. This contrasts the trends observed for both HOMO and LUMO of their tricarbonyl analogues (**2a-f**). On average, while the LUMO orbitals of **3a-f** remain at similar energies compared to **2a-f**, the HOMO orbitals are ∼1 eV higher in energy (making the HOMO–LUMO gap correspondingly smaller). These results are in line with the similar reduction potentials observed on both series, and the significantly lower oxidation potential of the dicarbonyl complexes. Orbital energy diagrams are shown in Figure S7 in the SI.

Apart from the significant change in the electronic density around the Re(I) centre introduced by replacing a C≡O ligand for a pyridine ligand (evidenced by the large red shift of all IR absorption bands), the local symmetry of the orbitals around the metal centre is increased when going from the κ^2N to the κ^3N geometry. Planarisation of the terpy ligand generates also a significant increase in conjugation, which now spans across the the three aromatic rings of the terpy ligand (also evidenced in the crystal structures of these complexes). This geometrical change suffices to introduce additional electronic transitions, evidenced by inspecting the UV-Vis absorption spectra (Figure 3A), and reproduced by TD-DFT calculations (Figure S5 in the SI).

The charge density difference (CDD) isosurfaces of complexes **3d-f** further support the observed TRIR results: no significant character change was observed when going from the unsubstituted terpy ligand (R^1 = H, **3d**) to the ligand substituted with the most electron-donating group (R^1 = NMe_2, **3f**). This contrasts with the case of the tricarbonyl complex **2f**. The CDD isosurfaces for the $S_1 \leftarrow S_0$ transitions of **2a-f** and **3d-f**, calculated with *MultiWfn* version 3.7,[59] are shown in Figure 9 as representative examples.

Two parallel effects—increased electron density and local symmetry—explain the more complex UV-Vis absorption spectrum of the dicarbonyls, and the red shift of ca. 1.55 eV in the energy of the $S_1 \leftarrow S_0$ transition. We attribute ca. 1 eV of this shift to the increase in the HOMO relative energies, and the remainder to the increased conjugation. Furthermore, we believe the increased electron density on the $\{Re(CO)_2\}^+$ moiety compared to the $\{Re(CO)_3\}^+$ core hinders charge transfer from the NMe_2 group, as the former is a more potent donor in the excited state.

The impact of the increased local symmetry around the metal centre in the dicarbonyl complexes **3a-f** can be further evidenced in the CDD isosurfaces of the higher excited states ($S_n \leftarrow S_0$), shown in Figure 10.

The fact that the CDD isosurfaces bear strong similarities results from the increase in the local symmetry of the complexes, and also serves to illustrate that these higher excited states have all an MLCT character.

The computational results presented herein serve to explain the observed changes in the electronic structure of these complexes when going from the κ^2N-tricarbonyl to the κ^3N-dicarbonyl coordination geometry. In addition, the limitations of the excited-state switching strategy (to avoid the energy gap law), towards increasing the lifetime and red shifting the absorption, are dissected in terms of symmetry and conjugation.

CONCLUDING REMARKS

Herein we studied the ground- and excited-state properties of a series of rhenium(I) dicarbonyl complexes with substituted 4'-(4-R^1-phenyl)-2,2':6',2"-terpyridine ligands in a κ^3N coordination motif, by employing a combination of ultrafast and steady-state spectroscopic

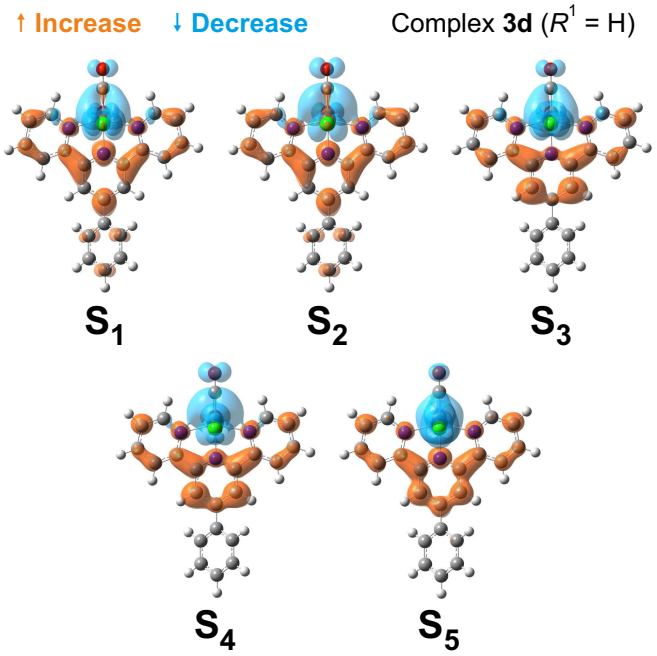

Figure 10. Charge density difference (CDD) isosurfaces of the $S_n \leftarrow S_0$ transitions for the first 5 singlet states of complex **3d**, shown at $|\Delta\rho| = 0.001$ a.u.

methods ranging from transient IR to IR spectroelectrochemistry, and density functional theory calculations.

In contrast to our previous report on analogous $\kappa^2 N$-tricarbonyl complexes,[40] we did not observe excited-state character switching when increasing the electron donating strength of the substituent from CN to NMe_2. In the present case, all excited states preserved their MLCT character, as evidenced by TRIR spectroscopy, and supported by TD-DFT calculations. The photophysical and electrochemical properties of these complexes showed excellent linear correlations with the Hammett σ_p substituent constants, in line with the results observed for their $\kappa^2 N$-tricarbonyl analogues operating from an MLCT excited state (**2a-e**).

TD-DFT calculations revealed the fundamental differences in electronic structure between complexes of the two series. We show that a combination of destabilisation of the HOMO orbitals (by replacing one CO for a pyridine), and an increase in the conjugation length are responsible for the observed ca. 1.55 eV red shift in the absorption. This shift consequently lowers the excited state lifetimes according to the energy gap law. We also show that for the remote substitution strategy to switch the lowest excited state to ILCT character in the excited state, a third carbonyl is needed, as the electron-rich $\{Re(CO)_2\}^+$ moiety outcompetes the electron-donating power of the NMe_2 substituent, thus hindering the access to ILCT states in these complexes.

We believe that this work presents the boundaries of the MLCT to ILCT switching strategy to enhance the lifetimes and absorption properties of Re(I) carbonyl complexes. This represents fundamental insight into the rich photochemistry, photophysics, and electronic structure of Re(I) carbonyl complexes with substituted terpyridine ligands.

ASSOCIATED CONTENT

Supporting Information The Supporting Information is available free of charge at `https://pubs.acs.org/xxxx`.

Full experimental details, including synthetic procedures, characterisation details, crystallographic discussions, details about the transient absorption and electrochemistry experiments; UV-Vis absorption, NMR and FT-IR spectra of all complexes; IR spectroelectrochemical data; details of the computational calculations, and additional tables and figures. (PDF)

Accession codes

CCDC 2032842 (**3b**) and 2032841 (**3f**) contain the supplementary crystallographic data for this paper. These data can be obtained free of charge via `www.ccdc.cam.ac.uk/data_request/cif`, or by emailing `data_request@ccdc.cam.ac.uk`, or by contacting The Cambridge Crystallographic Data Centre, 12 Union Road, Cambridge CB2 1EZ, UK; fax: +44 1223 336033.

AUTHOR INFORMATION

Corresponding Author

* E-mail: Ricardo.FernandezTeran@gmail.com and Ricardo.Fernandez@chem.uzh.ch;

ORCID identifiers

Ricardo Fernández-Terán 0000-0002-4665-3520
Laurent Sévery 0000-0002-6546-379X

Funding Sources

This research was funded through the Swiss National Science Foundation (Sinergia Project CRSII2 160801/1, and AP Energy Grant PYAPP2 160586), and the University Research Priority Program for Solar Light into Chemical Energy Conversion (LightChEC) of the University of Zurich.

Notes

The authors declare no competing financial interest.

ACKNOWLEDGMENTS

We thank Prof. Dr. Peter Hamm and Prof. Dr. S. David Tilley for their valuable input and encouragement. Estefanía Sucre-Rosales is greatly acknowledged for her support in part of the computational calculations. We

also thank Olga Božović and Jeannette Ruf for proofreading the manuscript and providing helpful comments. Dr. Benjamin Probst-Rüd, Prof. Dr. Roger Alberto, Dr. Jan Helbing and Gökçen Tek are acknowledged for insightful discussions. Prof. Dr. Bernhard Spingler and Prof. Dr. Anthony Linden are acknowledged for helpful crystallographic discussions.

REFERENCES

(1) Yi, X.; Zhao, J.; Sun, J.; Guo, S.; Zhang, H. Visible light-absorbing rhenium(I) tricarbonyl complexes as triplet photosensitizers in photooxidation and triplet–triplet annihilation upconversion. *J. Chem. Soc. Dalt. Trans.* **2013**, *42*, 2062–2074.

(2) Patrocinio, A. O. T.; Frin, K. P.; Murakami Iha, N. Y. Solid state molecular device based on a rhenium(I) polypyridyl complex immobilized on TiO_2 films. *Inorg. Chem.* **2013**, *52*, 5889–5896.

(3) Gao, Y.; Sun, S.; Han, K. Electronic structures and spectroscopic properties of rhenium (I) tricarbonyl photosensitizer: $[Re(4,4'\text{-}(COOEt)_2\text{-}2,2'\text{-}bpy)(CO)_3py]PF_6$. *Spectrochim. Acta - Part A Mol. Biomol. Spectrosc.* **2009**, *71*, 2016–2022.

(4) El Nahhas, A.; Consani, C.; Blanco-Rodríguez, A. M.; Lancaster, K. M.; Braem, O.; Cannizzo, A.; Towrie, M.; Clark, I. P.; Záliš, S.; Chergui, M.; Vlček, A. Ultrafast excited-state dynamics of rhenium(I) photosensitizers $[Re(Cl)(CO)_3(N,N)]$ and $[Re(imidazole)(CO)_3(N,N)]^+$: Diimine effects. *Inorg. Chem.* **2011**, *50*, 2932–2943.

(5) Anfuso, C. L.; Snoeberger, R. C.; Ricks, A. M.; Liu, W.; Xiao, D.; Batista, V. S.; Lian, T. Covalent attachment of a rhenium bipyridyl CO_2 reduction catalyst to rutile TiO_2. *J. Am. Chem. Soc.* **2011**, *133*, 6922–6925.

(6) Liu, J.; Jiang, W. Photoinduced hydrogen evolution in supramolecular devices with a rhenium photosensitizer linked to FeFe-hydrogenase model complexes. *Dalt. Trans.* **2012**, *41*, 9700–9707.

(7) Abdellah, M.; El-Zohry, A. M.; Antila, L. J.; Windle, C. D.; Reisner, E.; Hammarström, L. Time-resolved IR spectroscopy reveals a mechanism with TiO_2 as a reversible electron acceptor in a TiO_2─Re catalyst system for CO_2 photoreduction. *J. Am. Chem. Soc.* **2017**, *139*, 1226–1232.

(8) Probst, B.; Guttentag, M.; Rodenberg, A.; Hamm, P.; Alberto, R. Photocatalytic H_2 production from water with rhenium and cobalt complexes. *Inorg. Chem.* **2011**, *50*, 3404–3412.

(9) Guttentag, M.; Rodenberg, A.; Kopelent, R.; Probst, B.; Buchwalder, C.; Brandstätter, M.; Hamm, P.; Alberto, R. Photocatalytic H_2 production with a rhenium/cobalt system in water under acidic conditions. *Eur. J. Inorg. Chem.* **2012**, *2012*, 59–64.

(10) Guttentag, M.; Rodenberg, A.; Bachmann, C.; Senn, A.; Hamm, P.; Alberto, R. A highly stable polypyridyl-based cobalt catalyst for homo- and heterogeneous photocatalytic water reduction. *Dalt. Trans.* **2013**, *42*, 334–337.

(11) Rodenberg, A.; Orazietti, M.; Probst, B.; Bachmann, C.; Alberto, R.; Baldridge, K. K.; Hamm, P. Mechanism of photocatalytic hydrogen generation by a polypyridyl-based cobalt catalyst in aqueous solution. *Inorg. Chem.* **2015**, *54*, 646–657.

(12) Rodenberg, A.; Orazietti, M.; Mosberger, M.; Bachmann, C.; Probst, B.; Alberto, R.; Hamm, P. Quinones as Reversible Electron Relays in Artificial Photosynthesis. *ChemPhysChem* **2016**, *17*, 1321–1328.

(13) Takeda, H.; Koike, K.; Inoue, H.; Ishitani, O. Development of an efficient photocatalytic system for CO_2 reduction using rhenium(I) complexes based on mechanistic studies. *J. Am. Chem. Soc.* **2008**, *130*, 2023–2031.

(14) Takeda, H.; Ishitani, O. Development of efficient photocatalytic systems for CO_2 reduction using mononuclear and multinuclear metal complexes based on mechanistic studies. *Coord. Chem. Rev.* **2010**, *254*, 346–354.

(15) Kumar, B.; Llorente, M.; Froehlich, J.; Dang, T.; Sathrum, A.; Kubiak, C. P. Photochemical and Photoelectrochemical Reduction of CO_2. *Annu. Rev. Phys. Chem.* **2012**, *63*, 541–569.

(16) Morimoto, T.; Nakajima, T.; Sawa, S.; Nakanishi, R.; Imori, D.; Ishitani, O. CO_2 capture by a rhenium(I) complex with the aid of triethanolamine. *J. Am. Chem. Soc.* **2013**, *135*, 16825–16828.

(17) Kou, Y.; Nabetani, Y.; Masui, D.; Shimada, T.; Takagi, S.; Tachibana, H.; Inoue, H. Direct detection of key reaction intermediates in photochemical CO_2 reduction sensitized by a rhenium bipyridine complex. *J. Am. Chem. Soc.* **2014**, *136*, 6021–6030.

(18) Schreier, M.; Gao, P.; Mayer, M. T.; Luo, J.; Moehl, T.; Nazeeruddin, M. K.; Tilley, S. D.; Grätzel, M. Efficient and selective carbon dioxide reduction on low cost protected Cu_2O photocathodes using a molecular catalyst. *Energy Environ. Sci.* **2015**, *8*, 855–861.

(19) Wrighton, M.; David, L. The Nature of the Lowest Excited State in Tricarbonylchloro-1,10-phenanthrolinerhenium(I) and Related Complexes. *J. Am. Chem. Soc.* **1974**, *96*, 998–1003.

(20) Luong, J. C.; Nadjo, L.; Wrighton, M. S. Ground and Excited State Electron Transfer Processes Involving fac-T ricarbonylchloro(1, 10-phenanthroline)-rhenium(I). Electrogenerated Chemiluminescence and Electron Transfer Quenching of the Lowest Excited State. *J. Am. Chem. Soc.* **1978**, *100*, 5790–5795.

(21) Luong, J. C.; Faltynek, R. A.; Wrighton, M. S. Competitive Radiative Decay and Metal-Metal Bond Cleavage from the Lowest Excited State of Triphenyltin-and Triphenylgermanium Tricarbonyl(1, 10-phenanthroline)Rhenium. *J. Am. Chem. Soc.* **1979**, *101*, 1597–1598.

(22) Hawecker, J.; Lehn, J. M.; Ziessel, R. Electrocatalytic reduction of carbon dioxide mediated by $Re(bipy)(CO)_3Cl$ (bipy = 2,2'-bipyridine). *J. Chem. Soc. Chem. Commun.* **1984**, *6*, 328–330.

(23) Kalyanasundaram, K. Photophysics, photochemistry and solar energy conversion with tris(bipyridyl)ruthenium(II) and its analogues. *Coord. Chem. Rev.* **1982**, *46*, 159–244.

(24) Juris, A.; Campagna, S.; Bidd, I.; Lehn, J. M.; Ziessel, R. Synthesis and photophysical and electrochemical properties of new halotricarbonyl(polypyridine)rhenium(I) complexes. *Inorg. Chem.* **1988**, *27*, 4007–4011.

(25) Worl, L. A.; Duesing, R.; Chen, P.; Ciana, L. D.; Meyer, T. J. Photophysical properties of polypyridyl carbonyl complexes of rhenium(I). *J. Chem. Soc. Dalt. Trans.* **1991**, 849–858.

(26) Ley, K.; Schanze, K. Photophysics of metal-organic π-conjugated polymers. *Coord. Chem. Rev.* **1998**, *171*, 287–307.

(27) Takeda, H.; Koike, K.; Morimoto, T.; Inumaru, H.; Ishitani, O. *Adv. Inorg. Chem.*; Academic Press, 2011; Vol. 63; pp 137–186.

(28) Blanco-Rodríguez, A. M.; Kvapilová, H.; Sýkora, J.; Towrie, M.; Nervi, C.; Volpi, G.; Záliš, S.; Vlček, A. Photophysics of Singlet and Triplet Intraligand Excited States in $[ReCl(CO)_3(1-(2-pyridyl)-imidazo[1,5-\alpha]pyridine)]$ Complexes. *J. Am. Chem. Soc.* **2014**, *136*, 5963–5973.

(29) Zarkadoulas, A.; Koutsouri, E.; Kefalidi, C.; Mitsopoulou, C. A. Rhenium complexes in homogeneous hydrogen evolution. *Coord. Chem. Rev.* **2015**, *304-305*, 55–72.

(30) Portenkirchner, E.; Schlager, S.; Apaydin, D.; Oppelt, K.; Himmelsbach, M.; Egbe, D. A.; Neugebauer, H.; Knör, G.; Yoshida, T.; Sariciftci, N. S. Using the Alkynyl-Substituted Rhenium(I) Complex (4,4'-Bisphenyl-Ethynyl-2,2'-Bipyridyl)$Re(CO)_3Cl$ as Catalyst for CO_2 Reduction—Synthesis, Characterization, and Application. *Electrocatalysis* **2015**, *6*, 185–197.

(31) Klemens, T.; Czerwińska, K.; Szlapa-Kula, A.; Kula, S.; Świtlicka, A.; Kotowicz, S.; Siwy, M.; Bednarczyk, K.; Krompiec, S.; Smolarek, K.; Maćkowski, S.; Danikiewicz, W.; Schab-Balcerzak, E.; Machura, B. Synthesis, spectroscopic, electrochemical and computational studies of rhenium(i) tricarbonyl complexes based on bidentate-coordinated 2,6-di(thiazol-2-yl)pyridine derivatives. *Dalt. Trans.* **2017**, *46*, 9605–9620.

(32) Schoonover, J. R.; Strouse, G. F. Time-resolved vibrational spectroscopy of electronically excited inorganic complexes in solution. *Chem. Rev.* **1998**, *98*, 1335–1355.

(33) Atallah, H.; Taliaferro, C. M.; Wells, K. A.; Castellano, F. N. Photophysics and Ultrafast Processes in Rhenium(I) Diimine Dicarbonyls. *Dalt. Trans.* **2020**, *49*, 11565.

(34) Smithback, J. L.; Helms, J. B.; Schutte, E.; Woessner, S. M.; Sullivan, B. P. Preparative routes to luminescent mixed-ligand rhenium(I) dicarbonyl complexes. *Inorg. Chem.* **2006**, *45*, 2163–2174.

(35) Morimoto, T.; Ishitani, O. Modulation of the Photophysical, Photochemical, and Electrochemical Properties of Re(I) Diimine Complexes by Interligand Interactions. *Acc. Chem. Res.* **2017**, *50*, 2673–2683.

(36) Kurtz, D. A.; Brereton, K. R.; Ruoff, K. P.; Tang, H. M.; Felton, G. A.; Miller, A. J.; Dempsey, J. L. Bathochromic Shifts in Rhenium Carbonyl Dyes Induced through Destabilization of Occupied Orbitals. *Inorg. Chem.* **2018**, *57*, 5389–5399.

(37) Black, D. R.; Hightower, S. E. Preparation and characterization of rhenium(I) dicarbonyl complexes based on the meridionally-coordinated terpyridine ligand. *Inorg. Chem. Commun.* **2012**, *24*, 16–19.

(38) Frenzel, B. A.; Schumaker, J. E.; Black, D. R.; Hightower, S. E. Synthesis, spectroscopic, electrochemical and computational studies of rhenium(i) dicarbonyl complexes based on meridionally-coordinated 2,2':6',2"-terpyridine. *Dalt. Trans.* **2013**, *42*, 12440–12451.

(39) Bulsink, P.; Al-Ghamdi, A.; Joshi, P.; Korobkov, I.; Woo, T.; Richeson, D. Capturing Re(I) in an neutral: *N,N,N* pincer Scaffold and resulting enhanced absorption of visible light. *Dalt. Trans.* **2016**, *45*, 8885–8896.

(40) Fernández-Terán, R.; Sévery, L. Living Long and Prosperous: Productive Intraligand Charge-Transfer States from a Re(I) Terpyridine Photosensitiser with Enhanced Light Absorption. *Inorg. Chem.* **2020**, *Accepted*, DOI: 10.1021/acs.inorgchem.0c01939.

(41) Tu, S.; Jia, R.; Jiang, B.; Zhang, J.; Zhang, Y.; Yao, C.; Ji, S. Kröhnke reaction in aqueous media: one-pot clean synthesis of 4'-aryl-2,2':6',2"-terpyridines. *Tetrahedron* **2007**, *63*, 381–388.

(42) Sévery, L.; Siol, S.; Tilley, S. Design of Molecular Water Oxidation Catalysts Stabilized by Ultrathin Inorganic Overlayers—Is Active Site Protection Necessary? *Inorganics* **2018**, *6*, 105.

(43) Compain, J. D.; Bourrez, M.; Haukka, M.; Deronzier, A.; Chardon-Noblat, S. Manganese carbonyl terpyridyl complexes: their synthesis, characterization and potential application as CO-release molecules. *Chem. Commun.* **2014**, *50*, 2539–2542.

(44) Carballo, R.; Losada-González, P.; Vázquez-López, E. M. Synthetic, spectroscopic and structural studies of the rhenium(I) dicarbonyl complexes of phosphite, phosphonite, and phosphinite ligands: *cis,mer*-$[ReBr(CO)_2\{PPh_{3-n}(OR)_n\}_3]$ (R = Me, Et; n = 1-3). *Zeitschrift fur Anorg. und Allg. Chemie* **2003**, *629*, 249–254.

(45) Sato, S.; Sekine, A.; Ohashi, Y.; Ishitani, O.; Blanco-Rodríguez, A. M.; Vlček, A.; Unno, T.; Koike, K. Photochemical ligand substitution reactions of *fac*-$[Re(bpy)(CO)_3Cl]$ and derivatives. *Inorg. Chem.* **2007**, *46*, 3531–3540.

(46) Morimoto, T.; Ito, M.; Koike, K.; Kojima, T.; Ozeki, T.; Ishitani, O. Dual emission from rhenium(I) complexes induced by an interligand aromatic interaction. *Chem. - A Eur. J.* **2012**, *18*, 3292–3304.

(47) Jurca, T.; Chen, W. C.; Michel, S.; Korobkov, I.; Ong, T. G.; Richeson, D. S. Solid-state thermolysis of a fac-rhenium(I) carbonyl complex with a redox non-innocent pincer ligand. *Chem. - A Eur. J.* **2013**, *19*, 4278–4286.

(48) Kiefer, L. M.; King, J. T.; Kubarych, K. J. Dynamics of rhenium photocatalysts revealed through ultrafast multidimensional spectroscopy. *Acc. Chem. Res.* **2015**, *48*, 1123–1130.

(49) Frisch, M. J. et al. Gaussian 16, Revision B.01. 2017; `http://gaussian.com/`.

(50) Hartl, F.; Vlček, A. Rhenium(I) Carbonyl Dioxolene Complexes: Electrochemical and Spectroelectrochemical (Resonance Raman, UV-visible and IR) Study of $[Re(CO)_3L(Diox)]^z$ and $[Re(CO)_2(PPh_3)_2(Diox)]^z$ (L = CO, PPh_3, P-DPPE, THF, Ph_3PO,Me_2CO, py; z = -1, 0, +1) Redox Series. *Inorg. Chem.* **1992**, *31*, 2869–2876.

(51) Ishitani, O.; George, M. W.; Ibusuki, T.; Johnson, F. P.; Koike, K.; Nozaki, K.; Pac, C.; Turner, J. J.; Westwell, J. R. Photophysical Behavior of a New CO_2 Reduction Catalyst, $Re(CO)_2(bpy)\{P(OEt)_3\}_2^+$. *Inorg. Chem.* **1994**, *33*, 4712–4717.

(52) Johnson, F. P. A.; George, M. W.; Hartl, F.; Turner, J. J. Electrocatalytic Reduction of CO_2 Using the Complexes $[Re(bpy)(CO)_3L]^n$ (n = +1, L=$P(OEt)_3$,CH_3CN; n=0, L=Cl^-,Otf^-; bpy=2,2'-Bipyridine; Otf^-=CF_3SO_3) as Catalyst Precursors: Infrared Spectroelectrochemical Investigation. *Organometallics* **1996**, *15*, 3374–3387.

(53) Mukherjee, J.; Siewert, I. Manganese and rhenium tricarbonyl complexes equipped with proton relays in the electrochemical CO_2 reduction reaction. *Eur. J. Inorg.*

Chem. **2020**, *Accepted*, DOI: 10.1002/ejic.202000738.
(54) Hamm, P.; Lim, M.; Hochstrasser, R. M. Vibrational energy relaxation of the cyanide ion in water. *J. Chem. Phys.* **1997**, *107*, 10523–10531.
(55) Hamm, P.; Kaindl, R. A.; Stenger, J. Noise suppression in femtosecond mid-infrared light sources. *Opt. Lett.* **2000**, *25*, 1798.
(56) Helbing, J.; Hamm, P. Compact implementation of Fourier transform two-dimensional IR spectroscopy without phase ambiguity. *J. Opt. Soc. Am. B* **2011**, *28*, 171.
(57) Cannizzo, A.; Blanco-Rodríguez, A. M.; Nahhas, A. E.; Šebera, J.; Záliš, S.; Vlček, A.; Chergui, M. Femtosecond fluorescence and intersystem crossing in rhenium(I) carbonyl-bipyridine complexes. *J. Am. Chem. Soc.* **2008**, *130*, 8967–8974.
(58) Sato, S.; Matubara, Y.; Koike, K.; Falkenström, M.; Katayama, T.; Ishibashi, Y.; Miyasaka, H.; Taniguchi, S.; Chosrowjan, H.; Mataga, N.; Fukazawa, N.; Koshihara, S.; Onda, K.; Ishitani, O. Photochemistry of *fac*-[Re(bpy)$(CO)_3$Cl]. *Chem. - A Eur. J.* **2012**, *18*, 15722–15734.
(59) Lu, T.; Chen, F. Multiwfn: A multifunctional wavefunction analyzer. *J. Comput. Chem.* **2012**, *33*, 580–592.

FOR TABLE OF CONTENTS ONLY

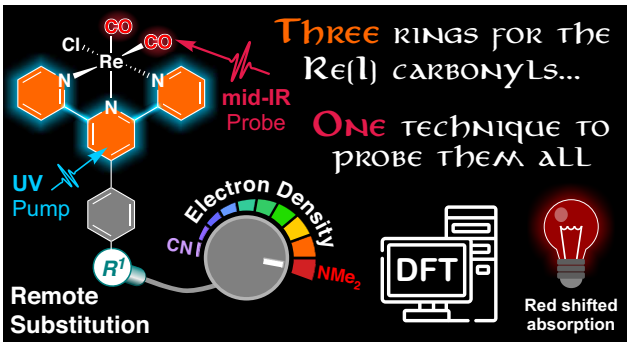

A series of Re(I) dicarbonyl complexes with κ^3N-coordinated 4'-(4-substituted-phenyl)-terpyridine ligands were studied with a range of experimental and computational methods. These complexes show panchromatic absorption, and are stronger photoreductants than their κ^2N-tricarbonyl counterparts—albeit with significantly shorter excited-state lifetimes. All dicarbonyls preserve an MLCT character in their lowest excited states, showcasing the boundaries of the remote substitution strategy towards long-lived and panchromatic photosensitisers.